Supplementary Information

Thermally Activated Delayed Fluorescence Chiral Molecules Exhibiting Photoinduced Radical Emission

Shujun Gong,[†a] Amjad Ali,[†b] Yudong Cao,[†c] Ying Liu,[*d] Glib V. Baryshnikov,[f, g] Hans Ågren,[bh] Guoquan Zhou,[*a] Yunhui Wan,[*a] Danfeng Ye,[*a] and Liangliang Zhu[e]

1. General

1.1 General Methods

All reactions were purchased from Aldrich and available chemicals were used without further purification. ^{1}H NMR and ^{13}C NMR spectra were acquired on a JEOL ECZ 400 MHz NMR spectrometer. High resolution mass spectra (HRMS) were recorded on a Matrix assisted laser desorption ionization-time of flight/time of flight mass spectrometer (5800). The emission spectra and the PL lifetime spectra were recorded on an FLS 1000 (Edinburgh Instruments). The photoluminescence quantum yields of solutions were measured on QM40 with an integrating sphere (φ 150 mm) from Photo Technology International, Inc. (PTI, USA). Single crystal X-ray diffraction signals were collected by a Bruker D8 Venture operating at room temperature. Transmission electron microscopy (TEM) was performed on a Jeol JEM 2100 with an accelerating voltage of 200 kV. Fourier transform infrared (FTIR) spectroscopy was carried out with a Thermofisher Nicolet 6700 spectrometer using KBr pellets as the sample matrix in the wavenumber range of 400-4000 cm^{-1}. Dynamic light scattering (DLS) experiments were carried out with Nano-Zeta Potential Analyzer ZS-90. Cell viability was tested using CCK-8 cell viability test kit. The photoluminescence images of 4T1 cells were acquired using a Lecia DMi8 photoluminescence microscopy (Leica, Germany).

1.2 Computational details

The chemical structures of neutral M1 and M2 molecules were primarily optimized at ground-state using density functional theory (DFT) with B3LYP[1, 2] functional and 6-31+G(d,p)[3, 4] basis set in a gas phase approximation. Based on the optimized geometries of neutral molecules, we optimized the chemical geometries at the ground doublet state (D0) for cation radicals of M1 and M2 molecules using the spin-unrestricted UB3LYP/6-31+G(d,p) theory level. We accomplished the state-specific optimization of fluorescent doublet excited states (D1, D2, and D3) of M1 cation radicals employing Tamm-Dancoff approximation (TDA) 5 at the time-dependent (TD) DFT/CAM-B3LYP/6-31G(d) level of theory to estimate the fluorescence energy and intensity for the cation radicals that are responsible for the experimentally observed photoinduced fluorescence of M1 compound. We also optimized the D1, D2, and D3 doublet excited states of M3 to know their excitation nature and to dig the reason behind its non-photo activeness in PMMA. For improved quantitative match between experimental measurements and computed energies of D0-D2 and D0-D3 emission, we performed TDA/TDDFT/ULC-wPBE/6-31G(d) calculations. The Grimme's dispersion correction was accounted in all the above-mentioned calculations at the GD3 level.[6] The Gaussian 16 software[7] was used to perform all the calculations.

2. Synthesis Procedures.

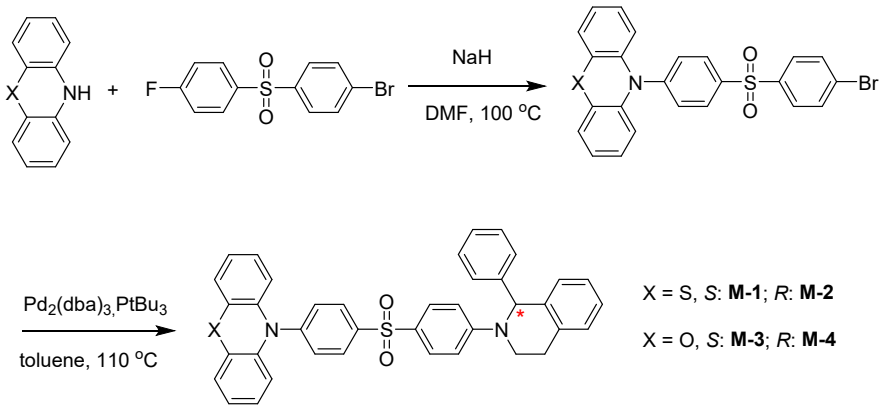

Scheme S1. Synthetic route of **M-1**, **M-2**, **M-3** and **M-4**

The compounds were synthesized according to the procedure reported. [7]

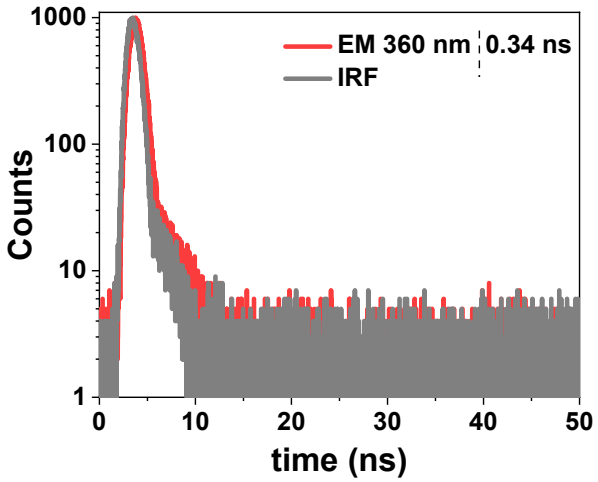

Figure S1. The lifetime decay spectra of 1% **M-1@PMMA** exhibited a prompt emission at 360 nm.

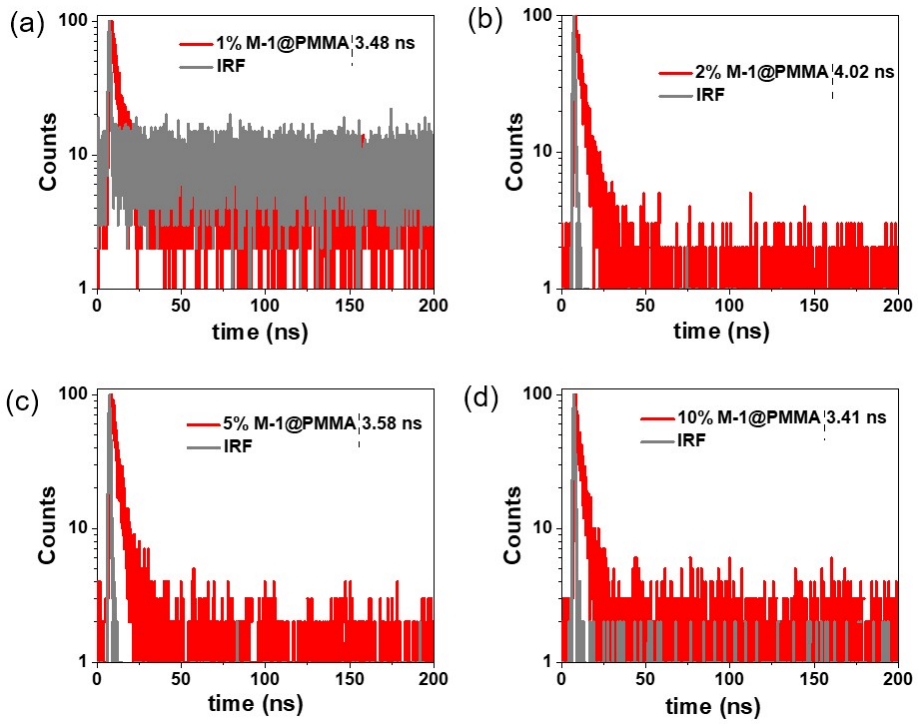

Figure S2. The lifetime decay spectra of 1-10% **M-1@PMMA**.

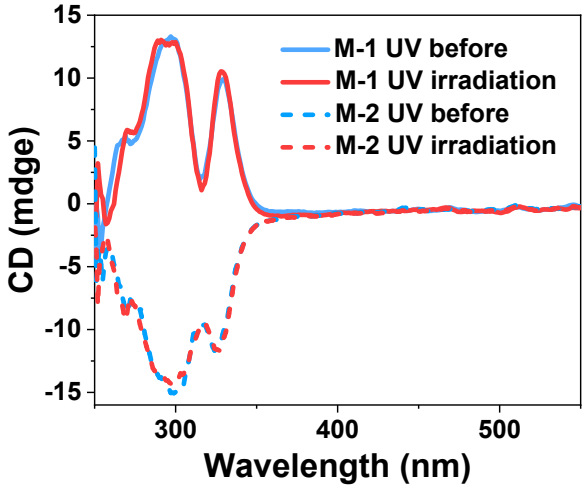

Figure S3. The CD signals of **M-1@PMMA** and **M-2@PMMA** film before and after UV irradiation.

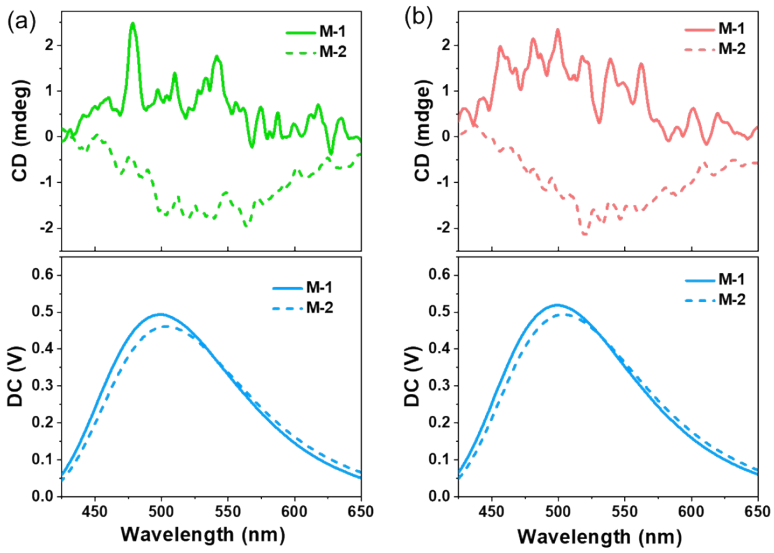

Figure S4. CPL spectra of **M-1@PMMA** and **M-2@PMMA** (a) before and (b) after irradiation.

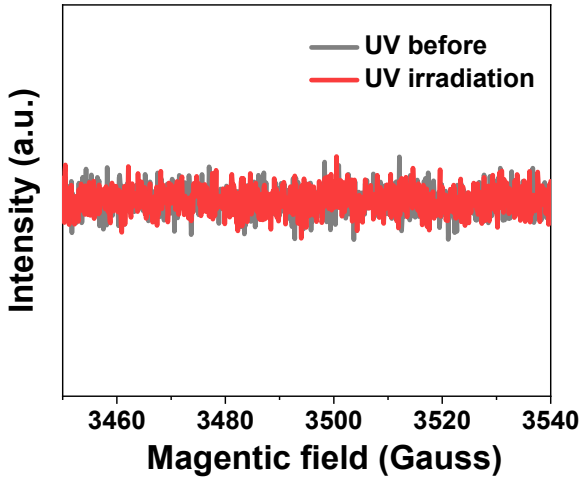

Figure S5. EPR spectra of **M-3@PMMA** before and after irradiation.

M-1 (Photoactive in PMMA)			
D0	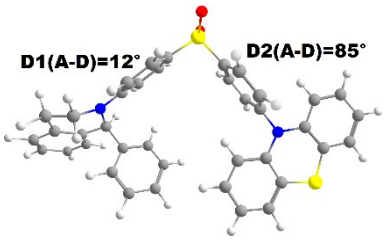	D1	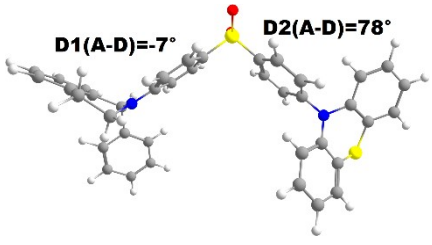

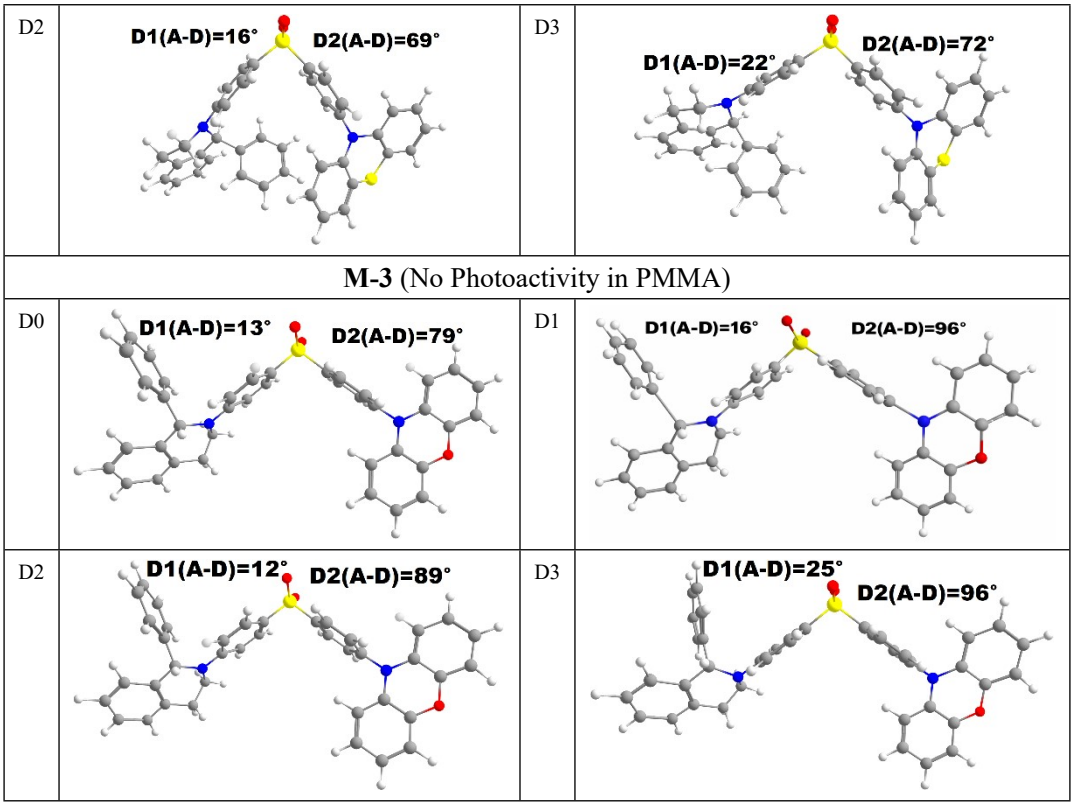

Figure S6. Optimized chemical geometries of D_0, D_1, D_2, and D_3 doublet-excited-states of **M-1** and **M-3** cationic radicals.

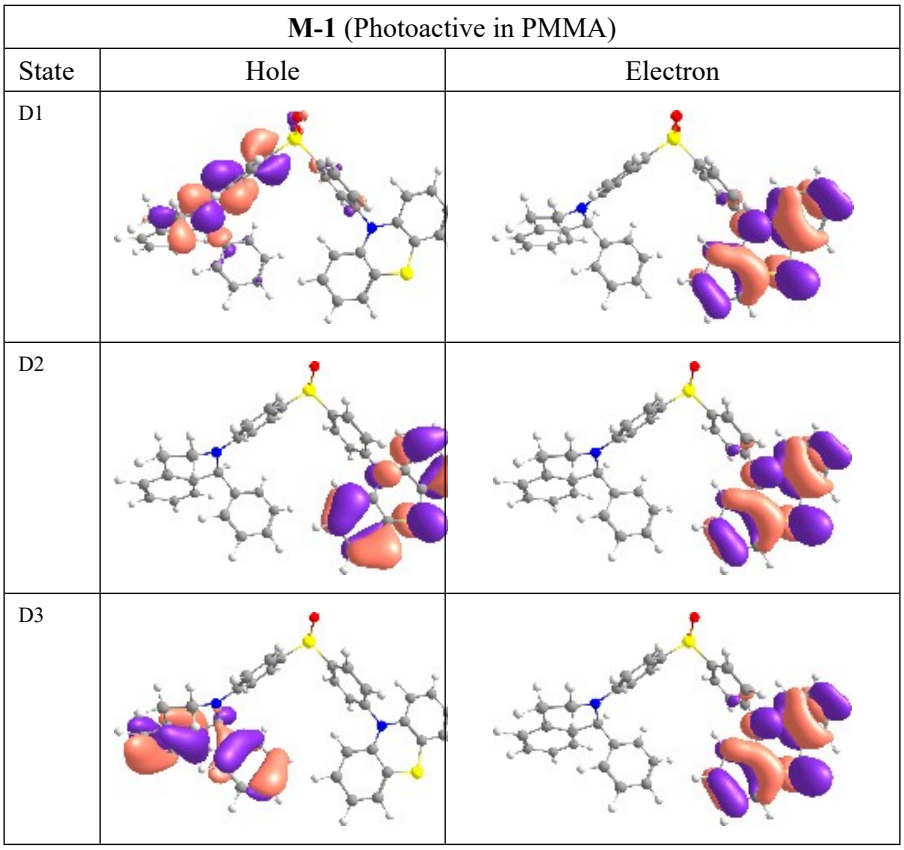

Figure S7. The hole and electron NTOs of optimozed D_1, D_2, and D_3 doublet-excited-states of **M-1** and **M-3** cationic radicals.

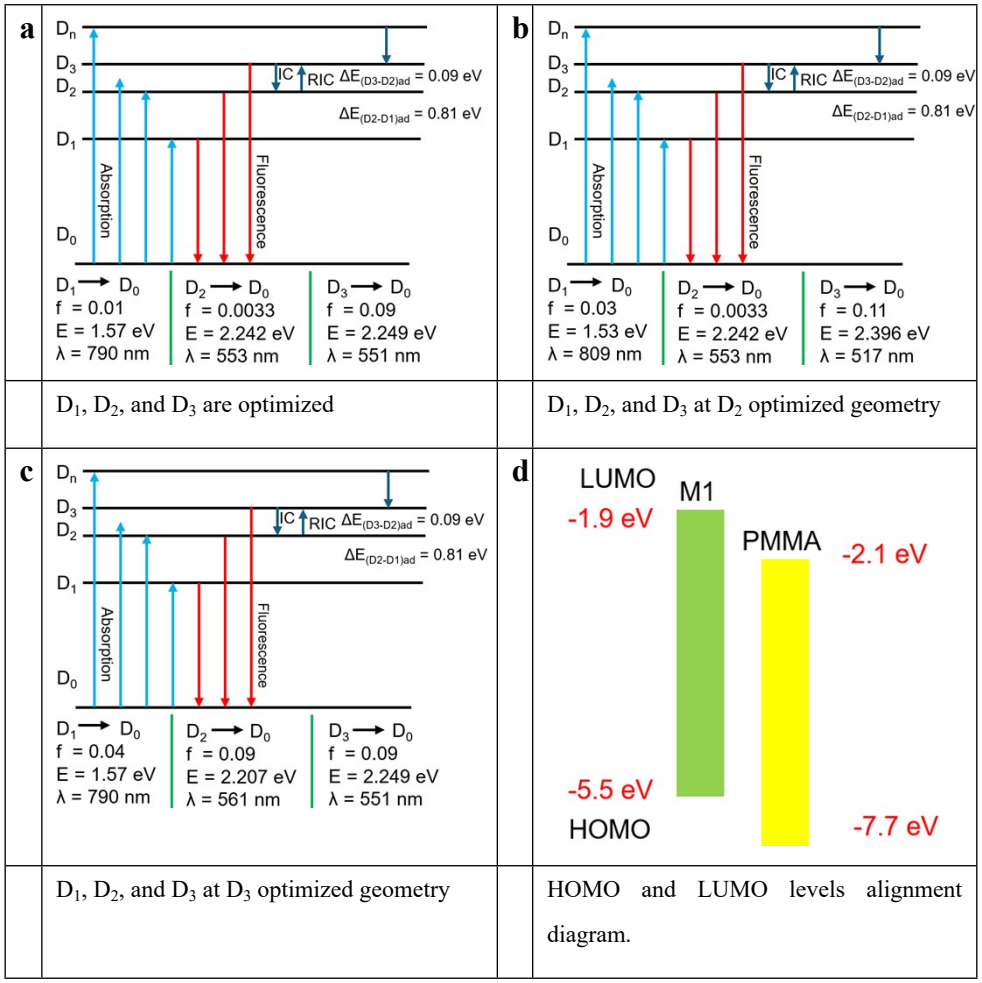

Figure S8. The hole and electron NTOs of optimozed D_1, D_2, and D_3 doublet-excited-states of **M-1** and **M-3** cationic radicals. Photophysical properties of **M-1** cation radical.

Table S1. Excitation Energy of the optimozed D_1, D_2, and D_3 doublet-excited-states of **M-1** cationic radicals. The oscillator strength is given in paranthesis.

D_1		D_2		D_3	
nm	eV	nm	eV	nm	eV
789.51 (0.01)	1.57	553 (0.0033)	2.242	551 (0.096)	2.249

Table S2. Excitation Energy of the optimozed D_1, D_2, and D_3 doublet-excited-states of **M-2** cationic radicals. The oscillator strength is given in paranthesis.

D_1	D_2	D_3
2123 (0.0)	742 (0.02)	671 (0.0)
1196 (0.0)	818 (0.02)	635 (0.0)
1116 (0.0)	741 (0.02)	1010 (0.0)

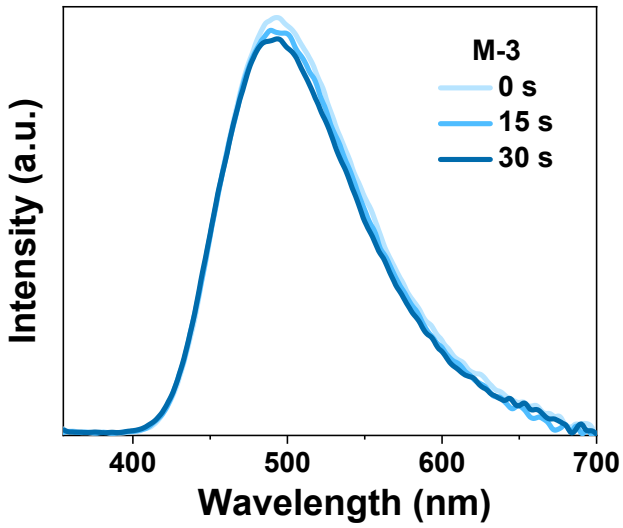

Figure S9. The PL spectra of the 1% M-3@PMMA film under UV irradiation.

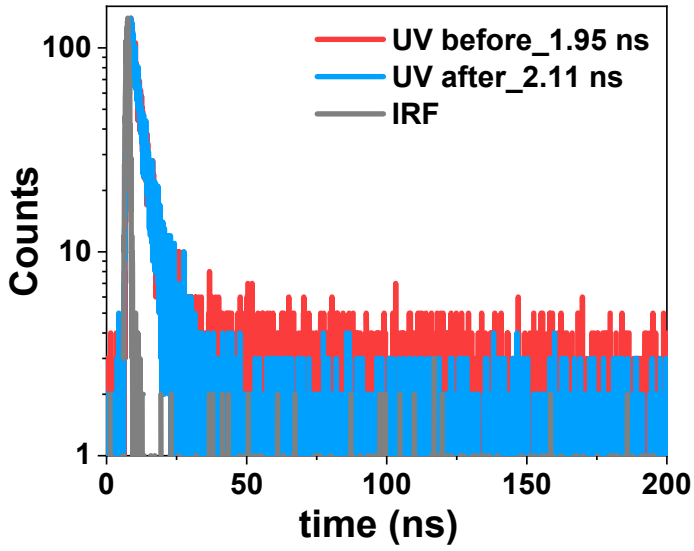

Figure S10. The PL spectra of the 1% **M-3@PMMA** film under UV irradiation.

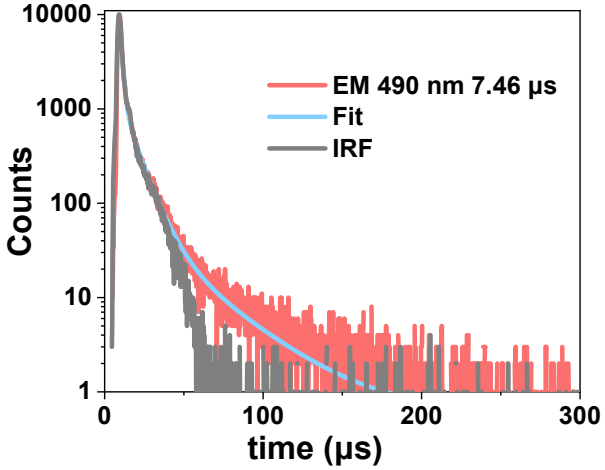

Figure S11. The decay lifetime spectra of the 1% **M-3@PMMA** film under UV irradiation.

References

(1) Becke, A. D. Density-functional thermochemistry. III. The role of exact exchange. *J. Chem. Phys.* **1993**, *98* (7), 5648-5652.

(2) Lee, C.; Yang, W.; Parr, R. G. Development of the Colle-Salvetti correlation-energy formula into a functional of the electron density. *Phys. Rev. B.* **1988**, *37* (2), 785.

(3) Ditchfield, R.; Hehre, W. J.; Pople, J. A. Self-consistent molecular-orbital methods. IX. An extended Gaussian-type basis for molecular-orbital studies of organic molecules. *J. Chem. Phys.* **1971**, *54* (2), 724-728.

(4) Frisch, M. J.; Pople, J. A.; Binkley, J. S. Self-consistent molecular orbital methods 25. Supplementary functions for Gaussian basis sets. *J. Chem. Phys.* **1984**, *80* (7), 3265-3269.

(5) Hirata, S.; Head-Gordon, M. Time-dependent density functional theory within the Tamm–Dancoff approximation. *Chem. Phys. Lett.* **1999**, *314* (3-4), 291-299.

(6) Grimme, S.; Antony, J.; Ehrlich, S.; Krieg, H. A consistent and accurate ab initio parametrization of density functional dispersion correction (DFT-D) for the 94 elements H-Pu. *J. Chem. Phys.* **2010**, *132* (15), 154104.

(7) Ye, D.; Zheng, G.; Ali, A.; Baryshnikov, G. V.; Ågren, H.; Li, S.; Chai, X.; Zhu, L., Highly Efficient Aggregation-Induced Chiral TADF Molecules Exhibiting Prolonged Lifetime in Living Cells under Hypoxic Stress. *Adv. Opt. Mater.* **2024**, 12 (36), 2401844.